ELSEVIER

Thermochimica Acta 287 (1996) 327–342

thermochimica acta

Estimation of rate coefficients from the overall amount of material reacted at various scan rates

Fabio Rosso [a], Gian Piero Bernardini [b], Daniele Borrini [b], Costanza Danti [b], Giulio G. T. Guarini [c,*], Giuseppe Mazzetti [d]

[a] *Dip. Matematica "U. Dini", Università di Firenze, Firenze, Italy*
[b] *Dip. Scienze della Terra, Università di Firenze, Italy*
[c] *Lab Chimica Fisica delle Interfasi, c/o Dip. Chimica, Università di Firenze, via G. Capponi, 9 50121, Firenze, Italy*
[d] *Museo di Mineralogia e Litologia, Università di Firenze, Italy*

Received 6 November 1995; accepted 6 April 1996

Abstract

A method to evaluate the temperature dependence of the reaction rate from the variation of the amount reacted at the end of a number of experiments at various scan rates is deduced from the fundamental equations of DTA. The method was applied to the synthesis of Pääkkönenite and gave parameters in good agreement with those determined for the same reaction by using other experimental data and the differential method of Sharp and Wentworth. Furthermore, an empirical procedure previously used to get the same results is compared with the present elaboration. The parameters evaluated are reported and discussed.

Keywords: Conversion and scan rate; Kinetic parameters; Pääkkönenite; Thermal methods; Theoretical analysis

1. Introduction

When the rate of transformation does not increase rapidly enough with temperature (low activation energy), it may happen, unless the scan rate g is sufficiently low, that the time employed to cross a certain temperature interval is insufficient to complete the transformation. This is what happened in a study [1] of the pyrosynthesis of Pääk-

* Corresponding author. Fax: +55-244102; e-mail: guarini@lcfs.chim.unifi.it

PII S0040-6031(96)03006-7

könenite, Sb_2AsS_2, from stibnite, Sb_2S_3, and stibarsen, Sb_2As_3

$$\tfrac{2}{3}Sb_2S_3 + \tfrac{1}{3}Sb_2As_3 \rightarrow Sb_2AsS_2, \quad (1)$$

where the amount of stibnite which reacted (before its melting) in the overall transformation decreased upon increasing the scan rate. In these instances, it appears logical that there exists (perhaps in a restricted range of values of g, the reaction being complete below a certain g and not taking place measurably above another higher g) a proportionality between the amount transformed and the time spent at a certain temperature, or, equivalently, between reaction rate and scan speed. For transformations reaching completion at every g, this proportionality law has already been assessed [2,3]. When otherwise the transformation is incomplete, as in the present case, and the degree of conversion changes with g, the problem of evaluating the temperature dependence of the rate from such data may arise. Here we develop some considerations aiming at the solution of this problem. We also suggest a possible justification for an empirical approach previously used for this purpose [1]. Such a procedure consisted in evaluating the overall conversion rates at various g_k, simply dividing the amount transformed by the time spent to scan the whole temperature interval with rate g. Successively, the corresponding g-dependent temperatures T for the construction of Arrhenius-like diagrams were calculated for each g by adding g times s to the initial temperature T_i, s being an arbitrarily chosen time interval, constrained only by the inequality $T_i + gs \leq T_f$ (the final temperature at which (1) is completed). The diagrams showed good linearity ($R \geq 0.95$), and the parameters obtained this way compared well with the "kinetic" ones evaluated by means of a differential method [4] in which the specific reaction rate $[f(\alpha)]^{-1}\mathrm{d}\alpha/\mathrm{d}T$ is calculated using for $f(\alpha)$ the form proposed by Ginstling and Brounshtein (see Ref. [5]).

We stress here that since the Arrhenius coefficients deduced by means of the empirical procedure are independent of the mechanism of the reaction, in the present report we do not use the usual term "kinetic parameters" for them.

2. Experimental

The relevant data on the pyrosynthesis of Pääkkönenite were collected by a Netzsch STA 409 quantitative DTA apparatus, the reactants being sealed in stoichiometric amounts into the ad hoc quartz vials also used in previous experiments [6]. The use of such vessels significantly reduces the sensitivity of our apparatus; however the choice of these vessels is compulsory for the thermal analysis of these systems. Scan rates g in the range 0.2–1.5°C min^{-1} were used. For further experimental details, see Ref. [1].

3. Results and discussion

3.1. Data

A set of three representative thermal curves of the pyrosynthesis of Pääkkönenite recorded at different g values is reported in Fig. 1. The size of the peak corresponding to

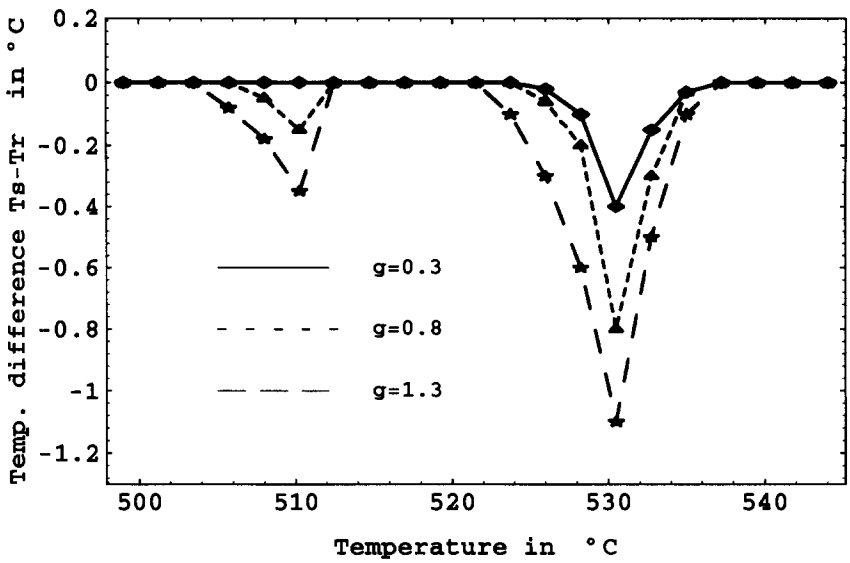

Fig. 1. Selected thermograms showing the variation of the melting peak of Sb_2S_3 with g at $\approx$ 510°C and the fusion of Sb_2AsS_2 at $\approx$ 530°C. Indicated points were selected from a series of readings taken from a strip chart.

the melting of stibnite at 510°C is seen to increase with g, indicating a decrease in the amount of stibnite consumed during the reaction. From the known value of the heat of fusion of stibnite, it was then possible to determine the overall fractional amounts of stibnite unreacted at various g (see in Table 1), i.e. the data that led to the above described empirical interpretation and to the present work.

Table 1
The change in curve parameters with increasing g

g/°C min^{-1}	T_i/°C	T_p/°C	ψ
0.2	100	460	0
0.3	75	455	0
0.4	130	440	0.018
0.5	80	450	0.035
0.7	115	435	0.083
0.8	102	457	0.0904
0.9	110	440	0.0999
1.2	137	467	0.16
1.3	140	460	0.17
1.4	120	450	0.18
1.5	125	450	0.23

3.2. Theory

Let us start by defining some useful quantities. To simplify notations within the analysis of reaction (1), we denote the reactants Sb_2S_3 and Sb_2As_3 by "A" and "B" respectively and the product Sb_2AsS_2 by "C".

We also denote by $m_X(t, g)$ the value of the mass of the component X at time t when the heating process takes place with constant heating rate $g = (dT/dt)$. Then, because of the principle of mass conservation and of the stoichiometric ratio γ, we have

$$m_A(t, g) + m_B(t, g) + m_C(t, g) = m_A(0, g) + m_B(0, g) = M, \quad \text{for all} \quad t \geq 0 \tag{2}$$

$$\frac{m_A(t, g)}{m_B(t, g)} = \gamma, \quad \text{for all} \quad t \geq 0 \tag{3}$$

The specific values of the above constants used in our experiments are $M = 1$ mole of C and $\gamma = 2$. The molecular weight of C is equal to 382.542.

As a consequence of (2) and (3), we get

$$m_C(t, g) = M - \left(1 + \frac{1}{\gamma}\right) m_A(t, g), \quad \text{for all} \quad t \geq 0 \tag{4}$$

Eq. (4) holds in particular for $t = t_f(g)$, the instant in which the reaction $A + B \rightarrow C$ virtually ends (no thermal activity can be detected by the instrument). Since all experiments are performed at constant heating rate, we have

$$t(T, g) = \frac{T - T_0}{g}$$

where T_0 is the initial temperature.

However, our observations show that the temperatures T_i at which the reaction starts show some dependence on the heating rate g (see Table 1). For the temperature T_p, at which the reaction reaches its peak, such a dependence is not evident, although it should be expected in consideration of the Arrhenius theory. The small range of g we considered, together with the experimental procedure used (silica vials), can account for the above. Furthermore, the temperature T_f, at which the reaction ends, seems to be practically independent of g and equal to $\simeq 480°C$.

Our data are rather noisy and a definite trend is hard to identify, although there seems to be a tendency of T_i to increase with g. We decided, in the spirit of a more general approach, to point out this expected dependence by writing, from now on, $T_i(g)$, $T_p(g)$ and $T_f(g)$ explicitly. Therefore, we have $t_i(g) = t(T_i(g), g)$ and similarly for $t_f(g)$. If we now write relationship (4) at $t = t_f(g)$ we get

$$m_C(t_f(g), g) = M - \left(1 + \frac{1}{\gamma}\right) m_A(t_f(g), g) \tag{5}$$

Experiments show that $m_A(t_f(g), g)$ increases with g; therefore Eq. (5) can be used to measure the "inhibitory effect" on the main reaction when a higher value of g is chosen.

Indeed it should be expected that for very high values of g, $m_A(t_f(g), g)$ will remain practically equal to its initial value $m_A(0)$, while for very small values of g, the whole mass $m_A(0)$ reacts with $m_B(0)$ to form $m_C(t_f(g), g)$. In other words, we introduce an "inefficiency" function $\psi(g)$ and write

$$m_A(t_f(g), g) = m_A(0)\psi(g) = \frac{\gamma M}{\gamma + 1}\psi(g) \tag{6}$$

where $\psi(g)$ can be identified by a "curve fitting" analysis and has to satisfy following limit conditions

$$0 \leq \psi(g) \leq 1$$

The relevant data are shown in Table 1. As shown in Fig. 2, ψ is practically linear for relatively small values of g.

Eq. (5) can also be used to measure both the specific and molar enthalpy of the process. Indeed we recall (see Refs. [7–9]) that if dH is the heat generated in the reacting sample during the interval of time dt, then

$$dH = C'_p d([\Delta T]_f - [\Delta T]_i) + K(T)\Delta T dt \tag{7}$$

Here K denotes the instrument calibration factor (see Fig. 3), $\Delta T = T_s - T_r$ the temperature gap between the sample and the reference, and C'_p the heat capacity of the empty reference and sample holders. (From now on the subscript "s" and "r" represent

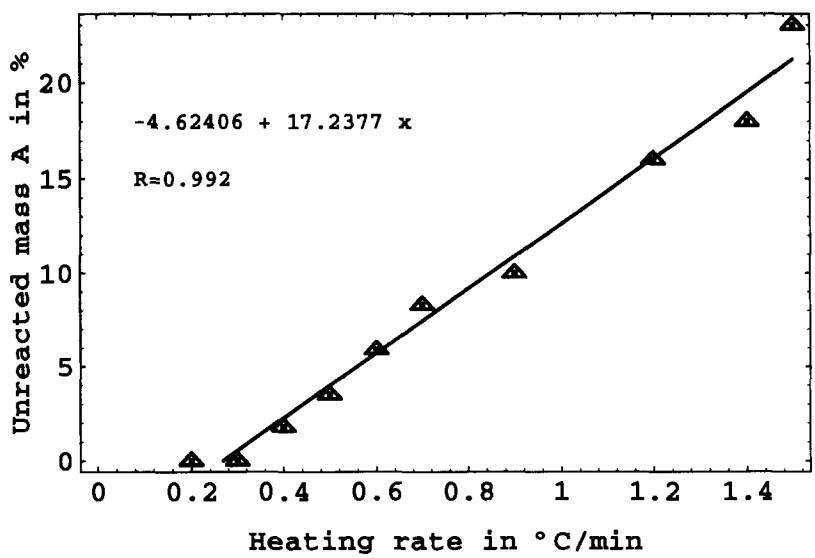

Fig. 2. The percentage of unreacted mass of A (stibnite) vs. the heating rate. Data refer to the measured area corresponding to the melting of A; this occurs at $\approx$ 510°C.

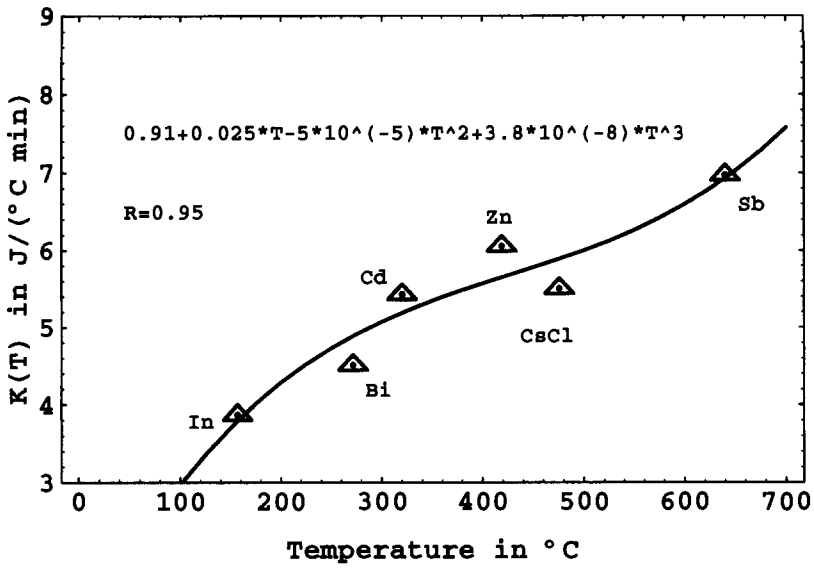

Fig. 3. Instrument calibration factor $K(T)$ in the temperature range used for experimental analysis. Points correspond to the instrument response when calibration elements or compounds, whose melting points and enthalpy changes are well known, are used. Tests performed at scan speeds of 0.2 and 1.0°C min^{-1} show essentially the same response.

"sample" and "reference" respectively, while "i" and "f" stand for "initial" and "final"). In our experiments, since $T(t, g) = gt + T_0$, the way K changes with time depends on the heating rate g; the functions ΔT also show a strict dependence on g (see Fig. 6). If we denote, for simplicity, ΔT by $h(t, g)$, an integration with respect to time of Eq. (7) yields

$$\Delta H = C'_p(h_f(g) - h_i(g)) + \int_{t_i(g)}^{t_f(g)} K(T(t, g))h(t, g)\mathrm{d}t \tag{8}$$

where $h_f(g) = h(t_f(g), g)$ and similarly for $h_i(g)$. In our experiments, we have $h_f(g) \simeq h_i(g)$; therefore, Eq. (8) is rewritten simply as

$$\Delta H = \int_{t_i(g)}^{t_f(g)} K(T(t, g))\, h(t, g)\mathrm{d}t \tag{9}$$

However (see Ref. [9], p. 164, Eq. (15)), one also has

$$\Delta H = m_C(t_f(g), g) \int_{(T_s)_i}^{(T_s)_f} C_p(T_s)\mathrm{d}T_s \tag{10}$$

where $C_p(T_s)$ is the heat capacity of the sample and, because of Eqs. (5) and (6)

$$m_C(t_f(g), g) = M(1 - \psi(g)) \tag{11}$$

Therefore the enthalpic change related with the process $A + B \rightarrow C$, appears to depend on g. Experimental data allow one to calculate, directly from Eq. (9), the enthalpic change of the sample and, dividing the result by $m_C(t_f(g), g)$, the specific enthalpy variation as well (see Table 2).

Fig. 4 shows a non-linear fitting curve of the pairs $(g, \Delta H_{sample})$. We obtained a rather high value of the regression coefficient ($R = 0.97$) by using powers of $1/g$: the fitting function turned out to be

$$\Delta H(g) = -0.63 + \frac{2.12}{g} - \frac{1.46}{g^2} + \frac{0.48}{g^3} - \frac{0.05}{g^4} \tag{12}$$

By means of Eqs. (10) and (11), we can also calulate the mean value $\hat{C}_p$ of $C_p(T)$ over the whole temperature range. Indeed we have

$$\hat{C}_p = \frac{1}{\Delta T_s} \int_{(T_s)_i}^{(T_s)_f} C_p(T_s) \mathrm{d}T_s = \frac{\Delta H}{M(1 - \psi(g))\Delta T_s(g)} \tag{13}$$

Fig. 5 shows data from Table 2 and a non-linear fitting curve of these data

$$C_p(g) = (30 - 15/g + 20/g^2 - 2.7/g^3) \times 10^{-4} \tag{14}$$

Fig. 6 shows some experimental thermograms; although h changes considerably with g, it remains essentially linear before and after the peak temperature $T_p(g)$. Symbolically this relationship can be expressed by

$$h(t, g) = \begin{cases} 0, & \text{if } 0 < t < t_i(g) \text{ or } t \geq t_f(g) \\ m(g)(t - t_i(g)), & \text{if } t_i(g) < t < t_f(g) - \varepsilon(g) \\ m(g)(t_f(g) - \varepsilon(g) - t_i(g))\dfrac{(t_f(g) - t)}{\varepsilon(g)}, & \text{if } t_f(g) - \varepsilon(g) < t < t_f(g) \end{cases} \tag{15}$$

Table 2
Enthalpy change and specific enthalpy variation with change in g

g/°C min^{-1}	ΔH_{sample}/kJ	ΔH_{spec}/kJ g^{-1}	$\hat{C}_p$/J g^{-1} °C^{-1}
0.2	1.851	0.00483	0.01273
0.3	1.734	0.00453	0.01119
0.4	0.904	0.0024	0.00687
0.5	1.012	0.00274	0.00685
0.7	0.344	0.00095	0.00261
0.8	0.752	0.00214	0.00567
0.9	0.384	0.00111	0.00301
1.2	0.461	0.00143	0.00418
1.3	0.364	0.00114	0.00318
1.4	0.268	0.000858	0.00237
1.5	0.238	0.00077	0.00228

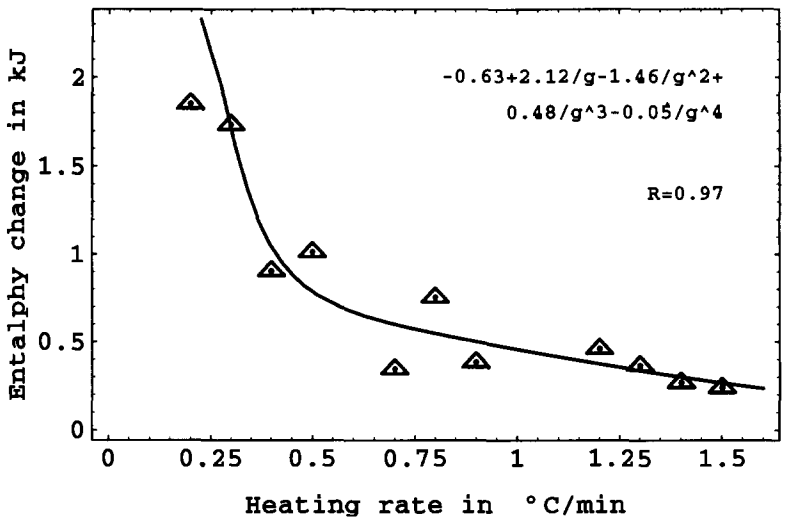

Fig. 4. Enthalpy change of the sample vs. g. Calculated points and a non-linear fitting curve are shown.

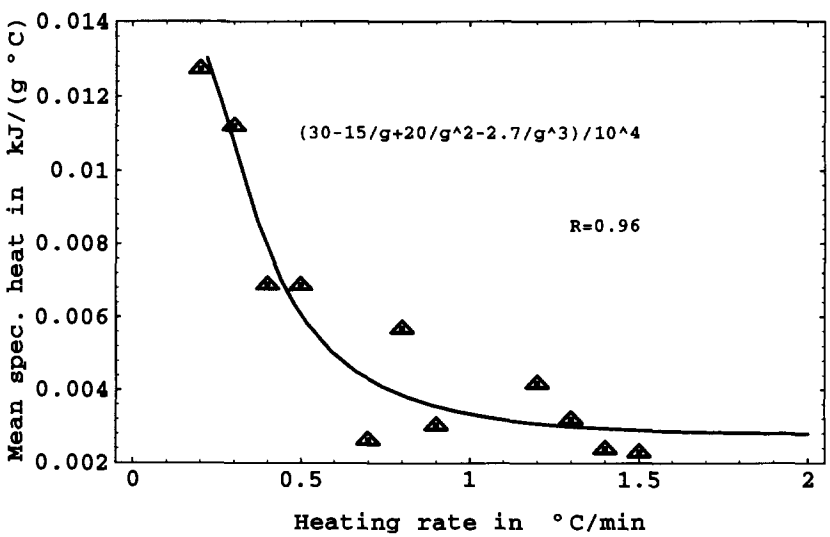

Fig. 5. Mean specific heat change of the sample vs. g. Calculated points and a non-linear fitting curve are shown.

Table 3
Experimental data

g/°C min^{-1}	E_a/kJ mol^{-1}	ln A	A/min^{-1}
0.2	57.75	2.24	9.45
0.3	50.75	1.21	3.36
0.4	69.49	3.40	30.18
0.5	56.09	1.39	4.05
0.7	66.2	1.28	3.63
0.8	55.34	1.01	2.75
0.9	56.24	−0.01	0.98
1.2	68.39	2.63	13.88
1.3	69.72	2.51	12.3
1.4	71.08	2.26	9.63
1.5	61.47	0.36	1.44

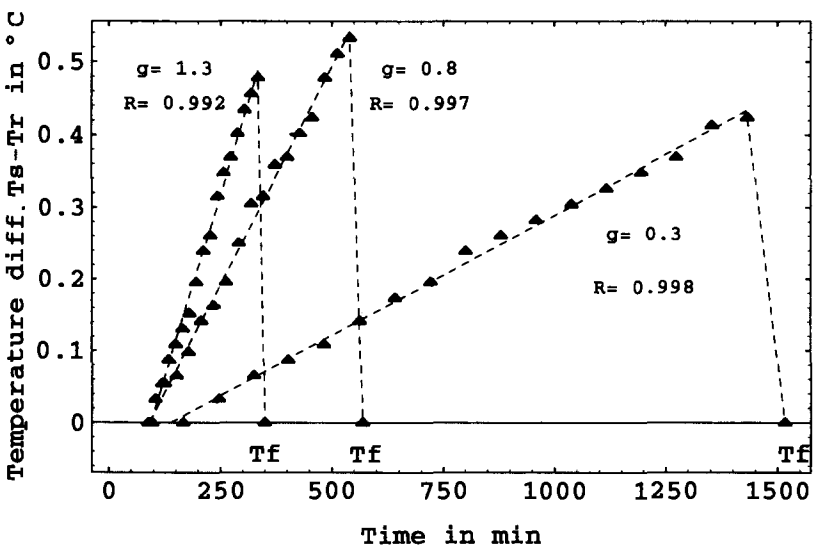

Fig. 6. Thermograms corresponding to the main reaction at different rates of the heating program.

where $\varepsilon(g)$ measures the lapse of time between $t_p(g)(=t(T_p(g),g))$ and $t_f(g)$. It is worth noticing that the values of the correlation coefficient R_{ht}, at least in the range of the g values considered, are rather close to 1 (Table 4).

The main point of this approach to the kinetic analysis is that we base our subsequent deductions upon the linearization of the key data h described by the above expression. Bearing in mind the table for R_{ht} at all g values, we feel very confident with

Table 4
Correlation coefficients, R_{hf}, at different g values

g/°C min^{-1}	R_{hf}
0.2	0.988833
0.3	0.998214
0.4	0.998634
0.5	0.994456
0.7	0.98121
0.8	0.997283
0.9	0.990119
1.2	0.99782
1.3	0.99743
1.4	0.990556
1.5	0.99233

this idea, which, by the way, has the advantage of minimizing all possible errors related to the calculation of the reaction velocity by means of numerical techniques.

We now define the fractional reaction, α, as

$$\alpha(t, g) = \frac{\int_{t_i(g)}^{t} h(s, g)\,\mathrm{d}s}{\int_{t_i(g)}^{t_f(g)} h(t, g_{\min})\,\mathrm{d}t} \tag{16}$$

where $g_{\min}$ is the lowest value of g used in the experiments. It should be noticed that our data definitely indicate $\int_{t_i(g)}^{t_f(g)} h(t, g)\mathrm{d}t \leq \int_{t_i(g)}^{t_f(g)} h(t, g_{\min})\mathrm{d}t$ for all g values. Therefore $\alpha(t_f(g), g)$ remains ≤ 1 for all g values.

We write the rate equation as

$$\frac{\mathrm{d}\alpha}{\mathrm{d}t} = \omega f(\alpha) \tag{17}$$

where, in the present instance, $f(\alpha)$ has the form proposed by Ginstling and Brounsthein for solid-state reactions based on diffusion mechanisms, i.e.

$$f(\alpha) = \frac{2}{3}[(1-\alpha)^{(-1/3)} - 1]^{-1} \tag{18}$$

Indeed at all values of g used in the experiments, the above form (18) of f is the one which turns out to offer the best fit of the Arrhenius-like plots to our data.

Of course, the specific reaction velocity ω depends on g: we set

$$\omega(t, g) = A(g)\exp\left[-\frac{E_a}{RT(t, g)}\right] \tag{19}$$

where, as usual, E_a denotes the activation energy (considered as a constant in the temperature range considered here), R the molar gas constant and A the pre-exponen-

tial factor. The logarithm of Eq. (19) is

$$\ln \omega(t, g) = \ln A(g) - \left(\frac{E_a}{R}\right)\frac{1}{T(t, g)} \tag{20}$$

Fig. 7 shows the pairs

$$\left(\ln\left(\frac{1}{f(\alpha)}\frac{d\alpha}{dt}\right), \frac{1000\,K}{T(t, g)}\right)$$

(calculated by using the functions (15), and Eqs. (16)–(18)), their linear fitting and their relevant regression coefficient. As one can see, the latter are all very close to 1.

If the reaction takes place by a single mechanism, E_a should not depend on g. Hence experimental data should agree with Eq. (20) in such a way that the slope remains practically constant while the intercept on the y-axis changes with g. This turns out to be sufficiently well verified in our case: indeed our E_a data do not show any correlation at all with g, thus showing that the oscillatory trend of E_a with g is essentially due to instrumental noise. Indeed we see from Table 3 that E_a has a mean value of about 62.05 ± 7.17 kJ mol^{-1} to be compared with 62.09 ± 9 kJ mol^{-1} obtained with the differential method [1].

The calculated values of $A(g)$ are also reported: it should be considered that, since data are concentrated in an interval of 1000 K/T whose range is about 1 and the lower bound of this interval is $\approx$ 1.5, small variations in the slope may generate significantly large variations in A (see also Ref. [10]). Anyway, both the low values and the dispersion of the data agree with the results of the kinetic analysis presented in Ref. [1]. The rough increase of E_a with g simulates the compensation effect [11, 12], also observed in Ref. [1].

4. Conclusions

From experimental data on the change of the overall amount of reactant transformed during the pyrosynthesis of Pääkkönenite, a method for evaluating kinetic parameters from such data has been developed and described. An analysis of the "Empirical Method" used in Ref. [1] is outlined in the Appendix.

Appendix A. Comparison of the "Empirical Method" with the present elaboration

A.1. The underlying idea

Considering now the empirical procedure used in Ref. [1] to evaluate the temperature coefficient of the rate from the overall conversion deduced by determining the amounts of stibnite reacted at various g, let us assume that the Arrhenius equation applies in the present instance and that the transformation does not change mechanism with g. Then for the values of the rate constant at any temperature $T(s, g) = T_i + gs$, we

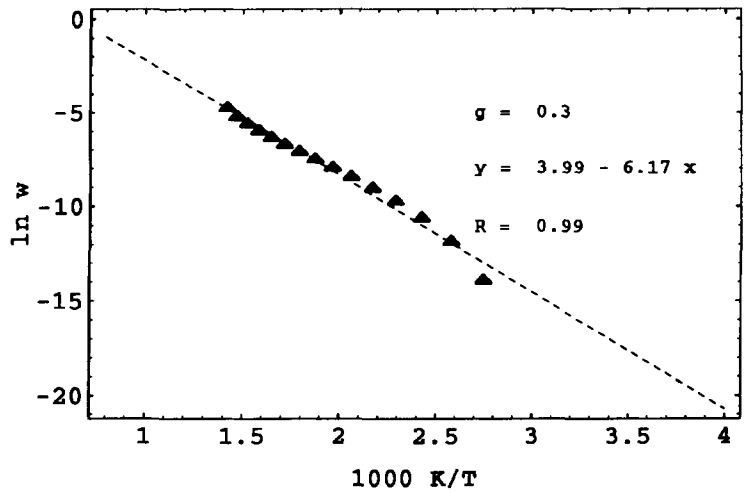

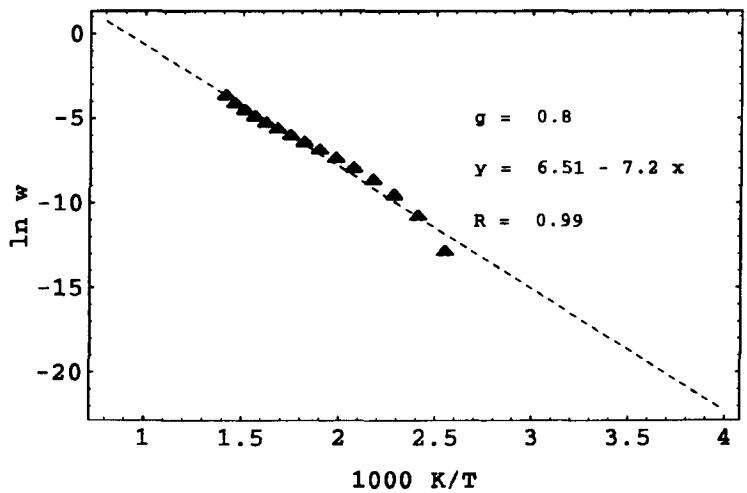

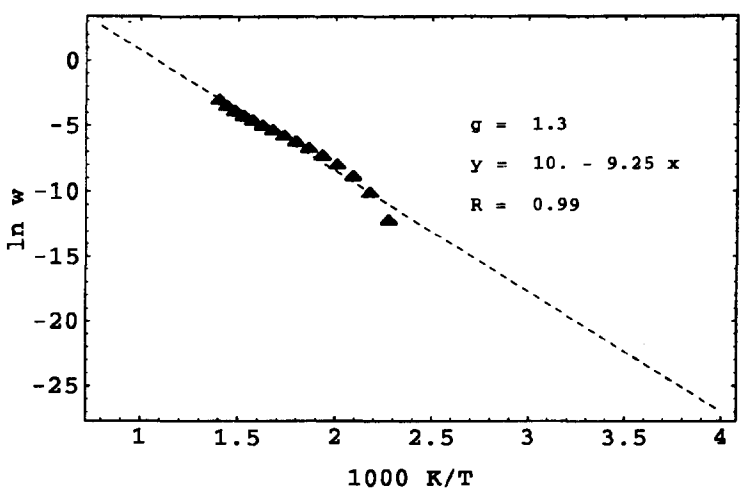

Fig. 7. Arrehenius-like plots at different values of g: temperature is measured in K

can write

$$k(T(s, g)) = A \exp\left[\frac{-E_a}{RT(s, g)}\right] \tag{A1}$$

where A and E_a are constants and s an arbitrary time interval. The empirical procedure used in Ref. [1] may be justified by considering the natural logarithm of Eq. (A1) when $T(s, g)$ can be reached in two different ways. Indeed in a variable temperature experiment, beginning at T_i and ending at T_f, any intermediate temperature $\bar{T}$ (and hence a defined value of the rate constant) can be reached either changing g for a given s or vice versa. The amount transformed "at" a certain temperature is proportional to the time spent in an infinitesimal temperature range centred at $\bar{T}$, i.e. $1/g$, so that the lower the scan rate the higher the amount transformed. However, using the two different ways to reach $\bar{T}$, the fraction transformed "up to" $\bar{T}$ will not be the same, thus giving different values of $f(\alpha)$ and hence of the rate of transformation. Anyway, in a certain interval of temperature the rate constant $k(T)$ will repeat the same set of values at each g; therefore the overall amount transformed will depend only upon $1/g$, and we can evaluate a rate of transformation averaged over the temperature interval by dividing the total amount transformed by the time $(T_f - T_i)/g$. If we consider a temperature $\bar{T}$, the amount transformed up to that temperature will likewise depend upon $(\bar{T} - T_i)/g$. Now if we take the arbitrary time interval s, the temperature reached after s units of time will be $\tilde{T} = T_i + gs$. The amounts transformed up to the various $\tilde{T}$'s, depending only on $1/g$, will be in the same ratios as the corresponding ones measured up to T_f. So, for each g, we can relate the overall averaged rate to the corresponding temperature T in order to construct Arrhenius-like diagrams.

However we must take into account that the selection of the value to be assigned to s is critical. Indeed, provided that Arrhenius plots, obtained from Eq. (A1) with s fixed and g variable, remain linear, the slope (and the intercept) of the line will change with s (because of the hyperbolicity of the temperature axis) simulating a compensation effect [11, 12]. For the present data, the best empirical value of s was approx. one tenth of the time taken to scan the total temperature interval at $g = 1°C\,min^{-1}$. Up to now we have no rational interpretation or can even guess at the reason for this value of s.

A.2. Theory

The "Empirical Method" developed in Ref. [1] needs to be compared with that presented in the previous subsection both from the point of view of theory as well as from that of the data. To begin with, we recall that the average velocity of the process (per unit mass) is defined as the overall reacted amount (in percentage) over the reaction time, i.e.

$$\bar{v}(g) = \frac{m_C(t_f(g), g)}{M\Delta t(T_f(g), g)} \tag{A2}$$

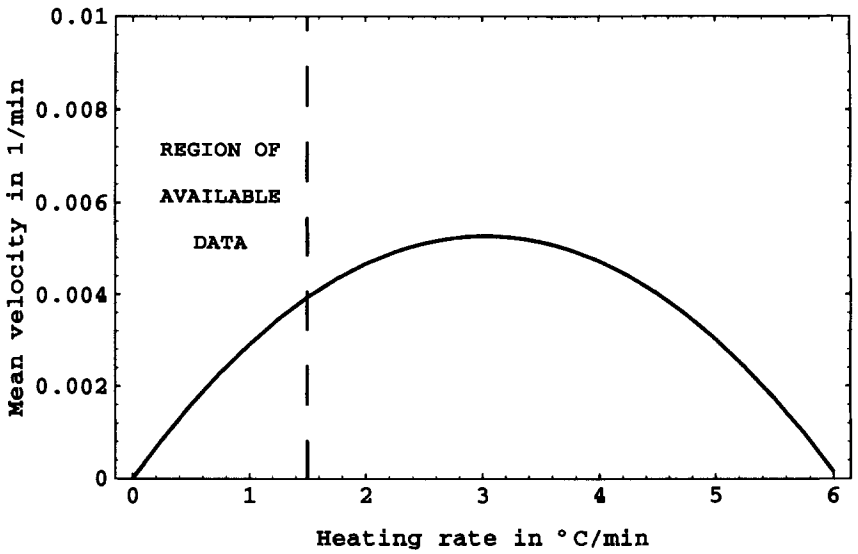

Fig. A1. Average velocity of the process vs. g. Our observations are, however, restricted within a small interval of g.

From Eq. (11), we may write $\bar{v}$ as

$$\bar{v}(g) = \frac{g(1-\psi(g))}{\Delta T_s(g)} \tag{A3}$$

In our experiments, $\Delta T_s(g)$ does not show a definite trend with respect to g; its mean value in $\overline{\Delta T} \approx 367°C$. If we use the mean value of $\Delta T(g)$ in Eq. (A3), then $\bar{v}$ has the pseudo-parabolic behaviour shown in Fig. A1. Although our observations are confined to a restricted range of values of g and $\psi(g)$ may not remain linear for higher values of g, the global behaviour shown by the graph seems to be physically significant since $\psi(g)$ must tend to 1 anyway for higher g's. Indeed by increasing g one leaves less and less time for the reaction to be completed; thus the overall amount is reduced to zero when the reaction has not even begun at the time the fusion temperature is reached

For the sake of simplicity, throughout this section we systematically use $\overline{\Delta T}$ instead of $\Delta T_s(g)$.

The "Empirical Method" rests upon the following fact: if we plot $y(g) = \log \bar{v}(g)$ versus $x(s, g) = 1000\,K/T(s, g)$, the pairs $(x(s, g), y(g))$ distribute along a straight line when g is allowed to vary in the range considered. As we recalled in the previous subsection, the slopes of these lines change with the choice of s; since the idea is to use the slope to determine the energy of activation of the process, the dependency on s is definitely an undesirable defect of the method unless some physically significant way to select one value of s among all possible ones is identified.

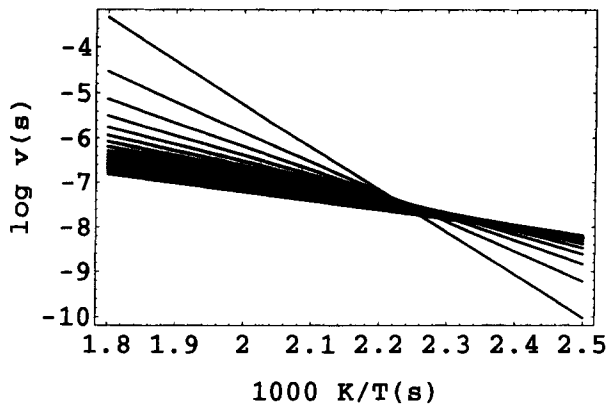

Fig. A2. Regression lines for the pairs $\{(1000\,K/T), \log \bar{v}\}$ parametrized with g; the steepest line corresponds to $s = 30$, the less steep one to $s = 300$

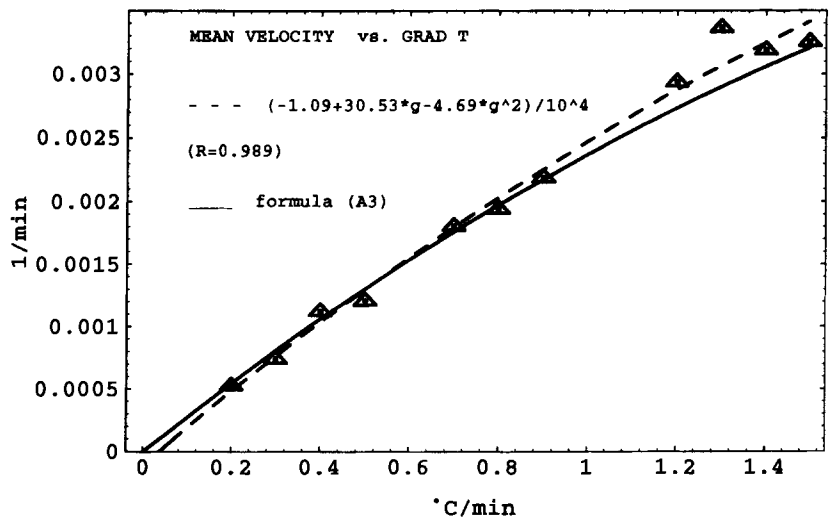

Fig. A3. The mean velocity $\bar{v}(g)$: points are obtained by using Eq. (A2) and experimental data; the dashed line is a quadratic fit of these data; the solid line uses the formula Eq. (A3).

The constraint $T(s, g) \leq T_f$ implies

$$0 \leq s \leq \frac{\overline{\Delta T}}{g}, \tag{A4}$$

Hence, for the present case, in principle s should not be chosen greater than $(\overline{\Delta T}/1.5) \simeq 244$.

Fig. A2 shows the above straight lines for several values of s; there are three facts worth pointing out:

(i) The regression coefficient $R(s)$ increases with s, always attaining values very close to 1 (≥ 0.958).
(ii) The straight lines meet at $(x_0(s), y_0(s))$ (see Fig. A2); $x_0(s)$ increases while $y_0(s)$ decreases with increasing s.
(iii) If $y = a(s) + b(s)x$ denotes the generic straight line, $a(s)$ and $b(s)$ behave as $-5.23 + (480.01/s)$ and $-0.94 + (184.39/s)$ respectively. Thus the limit line for $s = 244$ is $y = -3.2627 - 0.1843\,x$.

Since a rational interpretation for this method is still missing, we try to link the definition of $\bar{v}$ with the fractional reaction α defined by Eq. (16). By recalling relationships Eqs. (9)–(13), it is easily seen that

$$\bar{v}(g) = \frac{g}{M\hat{C}_p(\overline{\Delta T})^2}\int_{t_i(g)}^{t_f(g)} K(T(t,g))h(t,g)\,\mathrm{d}t = \frac{g\Delta H}{M\hat{C}_p(\overline{\Delta T})^2} \tag{A5}$$

Fig. A3 shows experimental points, their parabolic fitting and the function (A3). As can be seen, the agreement is satisfactory.

Acknowledgements

We wish to express our deep gratitude to both Referees for their constructive comments and suggestions. Financial support from both the University of Firenze (ex 60% MURST funds) and the G.N.F.M. of the National Research Council is also acknowledged.

References

[1] G.P. Bernardini, D. Borrini, F. Corsini, C. Danti, G.G.T. Guarini, G. Mazzetti and F. Rosso, Eur. J. Miner., 8 (1996) 639.
[2] T. Ozawa, Bull. Chem. Soc. Jpn., 38 (1965) 1881.
[3] H.E. Kissinger, Anal. Chem., 29 (1957) 1702.
[4] J.H. Sharp and S.A. Wentworth, Anal. Chem., 41, (1963) 2060.
[5] M.E. Brown, D. Dollimore and A.K. Galwey, Comprehensive Chemical Kinetics, Vol. 22, Elsevier, Amsterdam, 1990.
[6] G.P. Bernardini, C. Cipriani, F. Corsini, G.G.T. Guarini, G. Mazzetti and L. Poggi, Miner. Mag., 51 (1987) 295.
[7] H.J. Borchard and F. Daniels, J. Am. Chem. Soc., 79 (1957) 41.
[8] A. Lucci, in (Eds.) G. Della Gatta and A. Lucci Principi e applicazioni di calorimetria e analisi termica, Piccin, Padova, 1981.
[9] B. Wunderlich, Thermal Analysis, Academic, Press, Boston, 1990.
[10] R.R. Krug, W.G. Hunter and R.A. Grieger, Nature, 261 (1976) 566.
[11] A.K. Galwey, Adv. Catal., 26 (1977) 247.
[12] S. Vyazovkin and W. Linert, Chem. Phys., 193 (1995) 109.